# Full-Scale Development of Lift Engine Inlets for the XV-4B Aircraft

PAUL K. SHUMPERT* AND ANTHONY E. HARRIS†
*Lockheed-Georgia Company, Marietta, Ga.*

**An experimental investigation of lift engine inlet total pressure recovery and total and static pressure distortion during simulated hover and transitional flight has been conducted on a full-scale XV-4B model. The objectives were to develop fixed-geometry inlets for the four vertical-mounted lift engines that were independent of inlet closure door considerations and to provide satisfactory inlet pressure conditions for all modes of VTOL flight. The results indicate that satisfactory inlet pressures can be achieved with a design having single fixed auxiliary lips only in the forward inlets. Engine stalls, surges, and critical vibration levels were absent throughout the test program, which included numerous starts and accelerations at 200 knots relative wind speed. The total pressure recovery at static hover conditions was optimum, while total and static pressure distortions were always less than 13% and generally less than 10% in the VTOL transitional flight regimes for the final inlet configuration. A compact and flexible method of correlating inlet performance data is presented.**

## Nomenclature

| | | |
|---|---|---|
| $N$ | = | percentage of maximum engine compressor rotational speed, % rpm |
| $P$ | = | pressure, psia |
| $q$ | = | compressible dynamic pressure, psi |
| $T$ | = | temperature, °R |
| $V$ | = | velocity, knots |
| $W$ | = | inlet airflow rate, lb/sec |
| $\alpha$ | = | pitch angle (positive sign, nose up), deg |
| $\beta$ | = | yaw angle (positive sign, nose right), deg |
| $\delta$ | = | ratio between inlet total pressure and sea level standard pressure, $\delta = \bar{P}_{t2}/14.69$ |
| $\theta$ | = | ratio between inlet total temperature and sea level standard temperature, $\theta = \bar{T}_{t2}/518.69$ (note $T_{t0} = \bar{T}_{t2}$) |
| LSP | = | local static pressure $(P_{s2L} - P_{s0})$ |
| LSPC | = | local static pressure coefficient $(P_{s2L} - P_{s0})/\bar{q}_2$ |
| LTPL | = | local total pressure loss $(P_{t0} - P_{t2L})$ |
| LTPLC | = | local total pressure loss coefficient $(P_{t0} - P_{t2L})/\bar{q}_2$ |
| SPDC | = | static pressure distortion coefficient $(P_{s2max} - P_{s2min})/\bar{q}_2$ |
| SPD | = | static pressure distortion $(P_{s2max} - P_{s2min})/\bar{P}_{t2}$ |
| TPDC | = | total pressure distortion coefficient $(P_{t2max} - P_{t2min})/\bar{q}_2$ |
| TPD | = | total pressure distortion $(P_{t2max} - P_{t2min})/\bar{P}_{t2}$ |
| TPLC | = | total pressure loss coefficient $(\bar{P}_{t0} - \bar{P}_{t2})/\bar{q}_2$ |
| TPL | = | total pressure loss $(P_{t0} - \bar{P}_{t2})/\bar{P}_{t2}$ |

### *Subscripts*

| | | |
|---|---|---|
| 0 | = | freestream conditions |
| 2 | = | conditions at instrumentation plane (2.5 in. above engine compressor entry plane) |
| $L$ | = | local |
| $s$ | = | static |
| $t$ | = | total |
| max | = | maximum indicated at instrumentation plane |
| min | = | minimum indicated at instrumentation plane |
| $\bar{P}$ | = | bar over symbol denotes area-weighted mean |

Presented as Paper 68-636 at the AIAA 4th Propulsion Joint Specialist Conference, Cleveland, Ohio, June 10–14, 1968; submitted June 21, 1968; revision received February 11, 1969. The authors wish to thank all those who contributed to this program.

* Research and Development Engineer, Specialist, Advanced Propulsion and Thermodynamics Department.

† Thermodynamics Engineer, Senior, Advanced Propulsion and Thermodynamics Department. Member AIAA.

## Introduction

THE design requirements for lift engine inlets in V/STOL aircraft are severe. This severity evolves because the lift engine must be installed with minimum weight, volume, and frontal area; because engine airflow must be decelerated from flight speed to a considerably lower inlet velocity and turned approximately 90°; because engine airflow must enter with minimized pressure loss and pressure distortion; and because an inlet system of simplicity and reliability must be provided to operate over a wide range of relative freestream velocities and engine power levels.

A number of experimental research workers[1–6] have approached these problems as related to the design of multiple lift engines in a pod. Studies reported in Refs. 1, 2, 4, and 5 all included tests of inlet configurations involving retractable scoop-type inlet closure doors; Simonetti[1] and Tolhurst and Kelly[4] used individual doors for each inlet; Tyson[2] and Lavi[5] used large doors for two or more inlets. The test results for all scoop-type inlet configurations indicated that pressure-operated louvers would be required in the door or that the door position should be varied as a function of freestream velocity to improve the inlet pressure recovery at low flight speeds and high engine powers. Wiles[3] developed a simple retractable cascade mounted ahead of the front inlet and single auxiliary lips for the remaining inlets in a multiple unit pod. Kirk and Barrack[6] tested three in-line fuselage-mounted vertical lift engines with a fixed auxiliary lip in each inlet similar to that developed by Lockheed[7] as reported in the present paper.

The present study was concerned with the development of lift engine inlets for the XV-4B aircraft, which would provide satisfactory inlet performance for all modes of VTOL flight. The use of ram air for in-flight engine starting was not a requirement since turbine impingement starting using lift-cruise engine compressor bleed air was to be incorporated; however, favorable windmill characteristics were desirable to minimize bleed air requirements. The inlet configurations tested in this program were designed to be independent of inlet closure door considerations and were developed on the premise that a fixed-geometry inlet would satisfy the requirements outlined above.

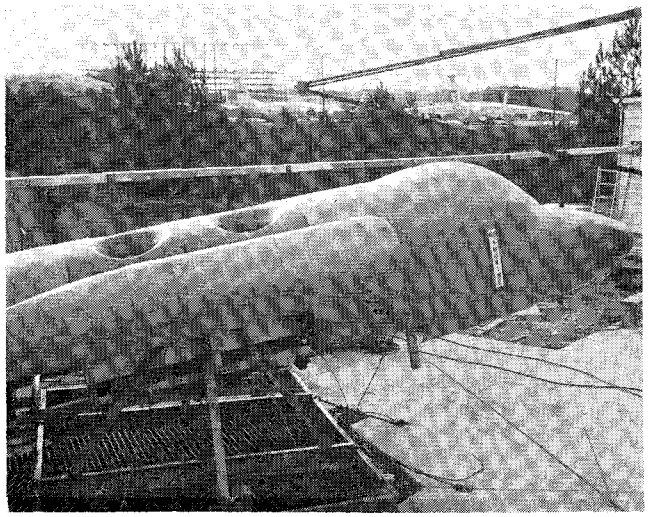

**Fig. 1 Model and test pad.**

## Model, Test Facility, and Instrumentation

### Model

The test model, as shown in Fig. 1, represented a full-scale simulation of the XV-4B aircraft front and center upper fuselage geometry and the cruise engine inlet and nacelle geometry. The model structure provided mounting points for the four vertically mounted GE YJ85-5 engines, which were located in a rectangular array with centerline spacings of 1.5 and 2.5 inlet throat diameters laterally and longitudinally, respectively. The complete model was mounted on a movable base which was anchored to the test pad at a number of points. Model position and yaw angle variations were made by translation and rotation of the complete model and base, whereas pitch angle changes were made by rotation of the model about a pivot fixed on the base.

The inlet was designed on the premise that acceptable performance could be obtained with a fixed-geometry minimum-weight design independent of inlet closure doors. The primary performance requirements of the inlet were to give optimum total pressure recovery in static operation and to give satisfactory levels of total and static pressure distortion throughout the operating envelope arising from transitional flight. To provide good static performance, a contraction ratio of at least 33% is required.[8] For the present inlet, the contraction ratio was designed to exceed this minimum. For high-speed flight operation the forward lip design is critical. To establish acceptable flow conditions behind this lip, a two-stage approach was adopted. The first was the design of a basic shape with a forward lip radius-to-inlet-diameter ratio of 47%; the second stage was the addition of an auxiliary lip designed to suppress separation on the forward lip.

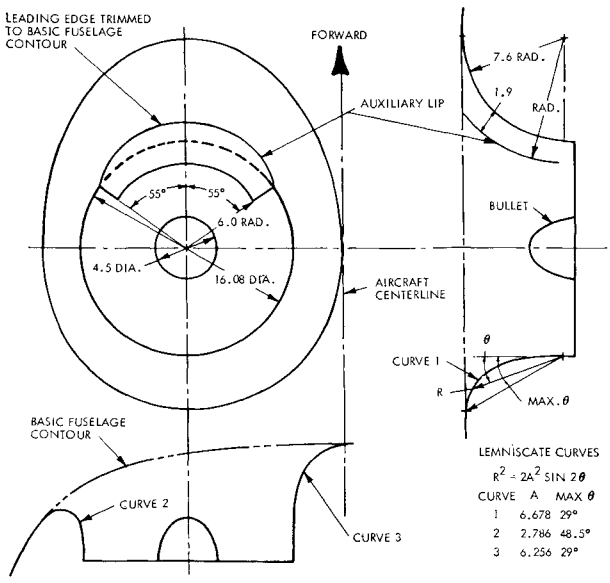


**Fig. 2 Basic inlet and auxiliary lip 3 geometry.**

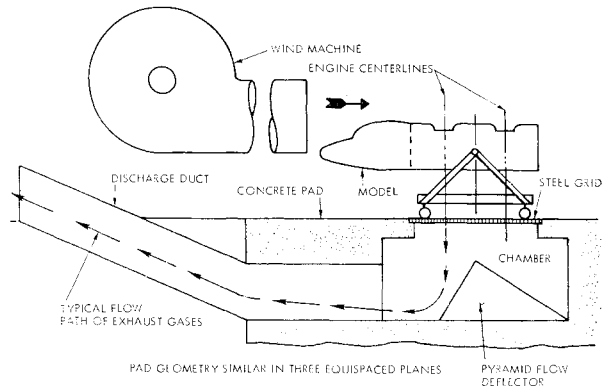


**Fig. 3 Schematic diagram of test pad.**

The basic inlet design, shown in Figs. 1 and 2, evolved from the above requirements, the constraints of the basic fuselage contours, and the data of previous experimental studies.[1–5] The auxiliary lip shown in Fig. 2 was designed to fit inside the basic fuselage contours and to give a ram scoop effect to unload the basic lip. Three designs of the auxiliary lip were fitted to the two forward inlets during the development program. The first design tested was a short lip fixed in such a position that the leading and trailing edges were approximately 3.2 and 2.0 in., respectively, from the basic lip. The second lip was mounted on two pivoting brackets near the trailing edge to allow the leading edge position to be varied and locked at a series of settings using a horn-type mounting fixed to the basic lip. The third and final lip design (Fig. 2) incorporated the optimum position determined from tests on lip 2 and was made from the same lip but with the mountings faired and fixed.

### Test Facility

Basically, the test facility consisted of a VTOL test pad, fuel system, wind machine, control room, and auxiliary equipment (engine start cart, electrical power supply, portable lights, and fire extinguishers). Of these items, the VTOL test pad and wind machine (Fig. 3) are of primary significance in the investigation reported herein.

The VTOL test pad consists of a concrete pad, a steel grid in the pad center opening, a concrete chamber beneath the pad center opening, and exhaust gas discharge ducts. The test pad was designed to collect the lift engine exhaust gases, divert the flows into three pairs of 5-ft-diam ducts, and discharge them at points remote from the engine inlets.

The wind machine was a 500,000 ft³/min centrifugal blower. The nozzle centerline was located at the same height as the model top surface in the zero-pitch attitude. The blower was fitted with a high-speed rectangular nozzle, 22 in. × 66 in. for simulation of wind speeds in the range of 80 to 200 knots, while lower wind speeds were created using the full 80-in.-diam circular nozzle.

### Instrumentation

Inlet instrumentation, located in each inlet as close to the engine entrance as practical, was designed to avoid engine-excited resonant frequencies. Total pressures, measured with eight rakes of four tubes each at area-weighted radii, were insensitive to flow angles of at least 20° with the probe head

**Table 1 Test program outline**

| $\beta$, deg | $\alpha$, deg | Nominal $V_0$[a], knots | Engine power, N |
|---|---|---|---|
| | | High-speed series | |
| 0, −15 | 10, 0, −10 | 120 | 48, 64, 90 |
| 0, −15 | 10, 0, −10 | 160, 180, 200 | 48, 64, 80, 90, 100 |
| 15 | 10 | 120 | 48, 64, 90 |
| 15 | 10 | 0, 160, 180, 200 | 48, 64, 80, 90, 100 |
| | | Low-speed series | |
| 0, −15 | 10, 0, −10 | 44 | 48, 64 |
| 0, −15 | 10, 0, −10 | 70, 94 | 48, 64, 90, 90, 100 |
| −45 | 10, 0, −10 | 34, 44 | 48, 64, 80, 90 |
| 90, −90 | 0 | 24, 31 | 48, 64, 80, 90 |

[a] In the high-speed section of the program, all engine starting and stopping performed with 200 knots nominal wind velocity.

design used. Four static pressure probes, essentially insensitive to flow angles up to 13°, were located (inboard, outboard, forward, and aft) at 94% of the inlet radius. Eight thermocouples with bare bead heads were used to measure total temperature. All inlet instrumentation was in the same plane.

## Test Program

A test program including combinations of lift engine power, relative freestream velocity, and aircraft attitude for the aircraft hover and transitional flight regime was developed from Ref. 9. The program, outlined in Table 1, was limited to those conditions likely to arise from steady controlled maneuvers and did not encompass all attitudes possible during unsteady flight. Some limits on combinations of engine power and freestream velocity were imposed due to the required total mass flow rates approaching the total wind machine flow rate. Separate test series were programmed employing the wind machine equipped with, first, the high-speed nozzle, and second, the larger low-speed nozzle.

Preliminary tests were run to determine wind machine freestream velocity profiles for the high-speed rectangular nozzle, both at the nozzle exit plane and at a station downstream of the nozzle exit corresponding to the location of the model inlets. The exit plane traverses indicated that the flow was substantially uniform at this location. Traverses of the windstream at the model location, which were obtained with the model removed, indicated that a high-velocity core was present in the windstream. This core was not large enough to envelope all four inlets. As a result, the model was located in positions such that particular fore-and-aft pairs of inlets were enveloped in the slipstream core. Model positions for all of the high-speed tests were determined as described and only the test data from those inlets in the slipstream core were evaluated. However, all four engines were operated at the nominal power settings indicated in Table 1 throughout the test program. With the low-speed nozzle, the velocity profiles were considerably fuller, and the model center was positioned on the wind machine centerline. It should be noted that throughout the tests, the relative freestream velocity was established at each inlet as described in the following section.

## Results and Discussion

### Reduction and Correlation of Results

The determination of freestream velocity presented a problem since the wind machine slipstream velocity was not completely uniform in either the cross-stream or streamwise directions due to diffusion of the wind machine slipstream. Also, changes in model attitude and engine power levels modified the manner in which the slipstream was deflected and ingested. It was required, therefore, to relate the performance of each inlet to the effective freestream velocity. The assumption was made, and later verified, that a region of full total pressure recovery would occur in all inlets at all test conditions. As a result, the freestream total pressure was determined from inlet total pressure probe readings. The pressure distributions were monitored throughout the program and only probes located in the interior of zero-loss regions were used for the determination of freestream total pressure.

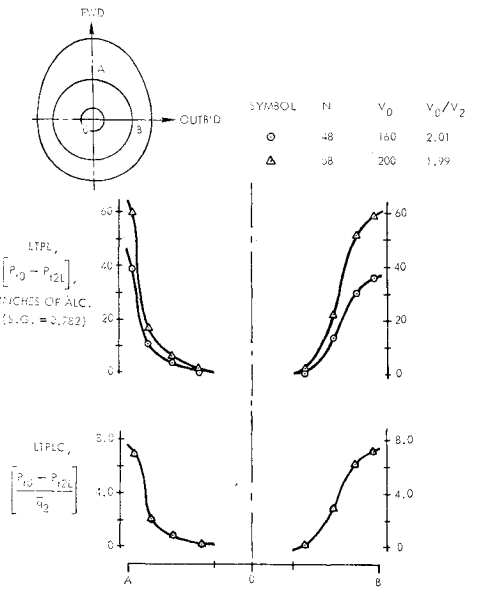


**Fig. 4 Radial distributions of local total pressure loss, forward inlet, basic configuration, $\alpha = 10°$, $\beta = 15°$.**

It will be noted that the test results are largely presented in the form of coefficients based on inlet mean dynamic pressure. The inlet airflow dynamic pressures and velocities used in the data reduction process were calculated from the engine airflow characteristic using a nominal 16-in.-diam inlet. The following reasoning led to the use of this method of correlation, which was found to be good within the limits of experimental error for all of the results obtained. It is argued that for a given model configuration and attitude, at a fixed freestream-to-inlet velocity ratio, the inlet flow pattern will

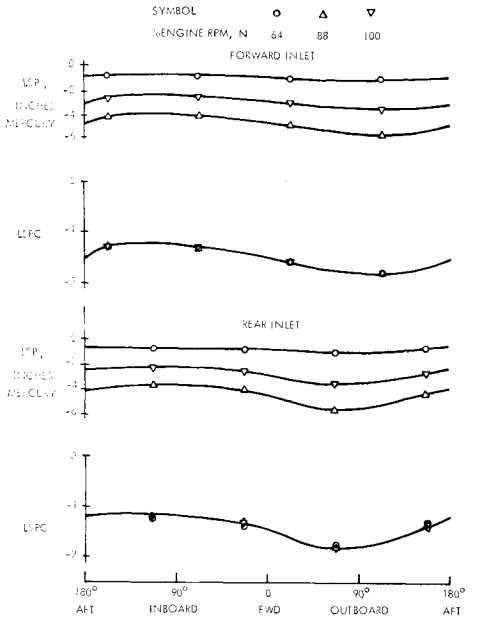


**Fig. 5 Circumferential distributions of static pressure, auxiliary lip 1 configuration, $V_0/V_2 = 0$.**

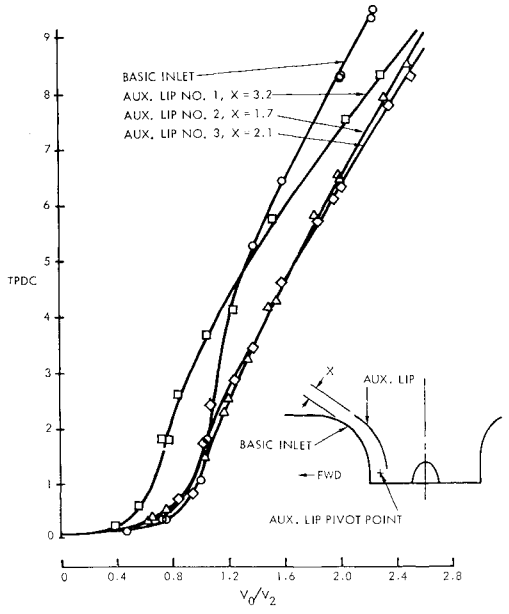


**Fig. 6 Comparison of total pressure distortion coefficients for preliminary configurations, right-side forward inlet, $\alpha = 10°, \beta = -15°$.**

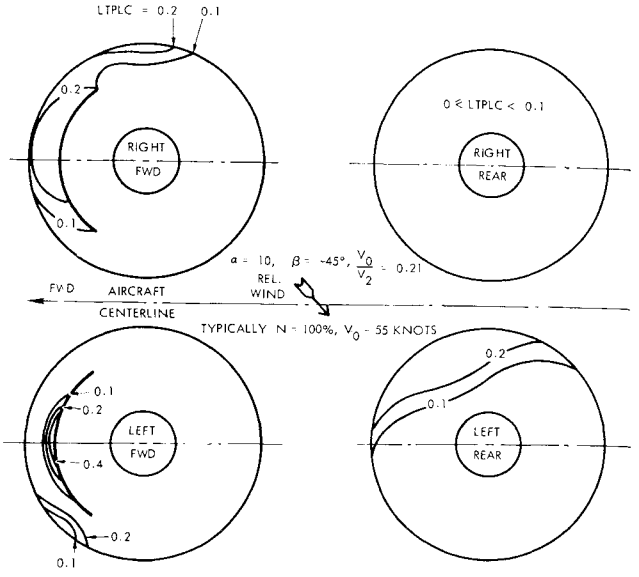


**Fig. 8 Total pressure loss distributions for all inlets at a typical low-speed flight condition with $\alpha = 10°, \beta = -45°$.**

be fixed provided that changes in the actual velocity levels do not modify the positions of any flow separation lines which may exist on any of the inlet surfaces. It is also argued that, should a separation region exist, the pressure losses occurring within this region will be dependent upon the dynamic pressure of the flow adjacent to this separation region. Further, since the flow is essentially subsonic, the dynamic pressure at any point will be proportional to some reference dynamic pressure, such as $\bar{q}_2$, for fixed $V_0/V_2$.

Some typical radial distributions of local total pressure loss and loss coefficient are shown in Fig. 4, and the pressure coefficient correlation is shown to be good. A typical set of circumferential plots of near-wall static pressure and LSPC are shown in Fig. 5 and again the correlation is demonstrated.

### Preliminary Inlet Configuration Test Results

Results obtained from tests on the basic inlet (Fig. 6) indicated that at zero wind velocity the pressure recovery was optimum. With $\alpha = 10°$, $\beta = -15°$, and speeds between 120 and 200 knots, however, the pressure distributions indicated that a separation region was developed on the forward lips of all inlets. This separation was caused by the severe adverse pressure gradients on these lips arising from the rapid diffusion and curvature of the inlet airflow. Figure 7 shows the location and size of the loss region caused by this separation at a typical high-speed test condition. A feature of this

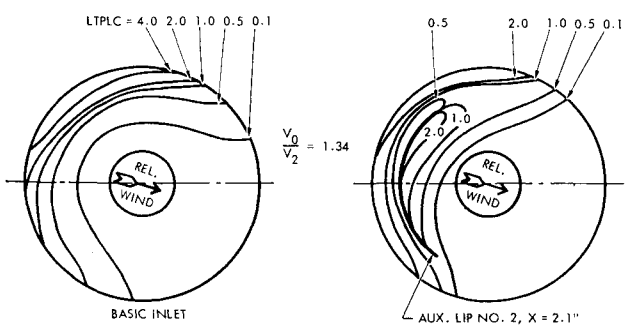


**Fig. 7 Total pressure loss distributions for two preliminary inlet configurations, right-side forward inlet, $\alpha = 10°, \beta = 15°$.**

distribution, and one which was found for all inlets and all configurations tested, is the region of zero loss in the rear of the inlet. In general, this zero-loss zone was located in the back of the inlet with respect to the relative windstream, as was to be expected. As a result of the separation region, TPD and TPL increased progressively with freestream speed at a fixed engine power setting. The magnitude of TPD was substantially in excess of the engine manufacturer's 10% limit and a configuration review led to the installation of auxiliary lip 1, which had been designed to suppress this separation, in the forward inlets. The decision on the fitting of auxiliary lips to the rear inlets was postponed as the preliminary test results indicated marginally acceptable distortion levels.

Tests with auxiliary lip 1 fitted (Fig. 6) showed that, although the basic lip flow separation was suppressed, a severe flow separation occurred at the auxiliary lip leading edge, and this again resulted in unacceptably high pressure distortions. The lip was positioned to produce a channel between it and the basic lip contracting from 3.2 in. clearance at the leading edge to 2.0 in. at the trailing edge. It appeared that this contraction was too strong and that a more nearly parallel channel might produce more desirable flow conditions. The reasons for this were that the inlet-to-approach streamtube area varied over a wide range, and that the high distortion levels were found to occur at the maximum freestream velocity in combination with moderate to low engine power levels. In particular, very high TPD's were obtained with $V_0 = 200$ knots in the range $1.2 \leqq V_0/V_2 \leqq 2.6$; in this range the inlet-to-approach streamtube area ratio varied from about 1.2 to 2.6. As a result of these considerations, the auxiliary lip design was modified to control the diffusion on the basic inlet leading lip. To provide this capability auxiliary lip 2 was built to allow the lip leading edge clearance to be reset between tests and thus provide variable channel contraction or expansion ratio. It was recognized that at the optimum fixed position of the lip, flow separations from the basic lip or the auxiliary lip would be likely to occur at off-design velocity ratios. The approach, however, was to minimize the distortions and eliminate all TPD's greater than 10% with a fixed auxiliary lip while maintaining substantially optimum recovery under static conditions.

Two test series were performed with auxiliary lip 2 with lip leading edge clearances of 1.7 and 2.1 in. and the results, which were similar, indicated significantly reduced TPD levels in the critical range. Figures 6 and 7 show that although a pair of high local loss regions did develop, they

were of reduced intensity and as a result the TPD levels were within the recommended 10% limit. Static tests with these configurations indicated very small reductions in total pressure recovery. Based on these test results the final lip was designed to give a leading edge clearance of 1.9 in. Further testing indicated that the performance of the clean rear inlets was acceptable.

### Final Inlet Configuration Test Results

The final inlet configuration had auxiliary lip 3 mounted on faired struts in both forward inlets but the rear inlets were clean.

Test results confirmed that with zero relative wind the pressure loss was substantially zero for all inlets in the final configuration. Tests simulating pure sideward motion ($\beta = -90°$) at speeds up to 40 knots indicated that losses in this condition were generally very small, not exceeding a LTPLC of 0.2. Tests with $\beta = -45°$ (Fig. 8) at speeds up to 55 knots indicated losses associated with the auxiliary lip and in addition an appreciable loss originated from the high aircraft

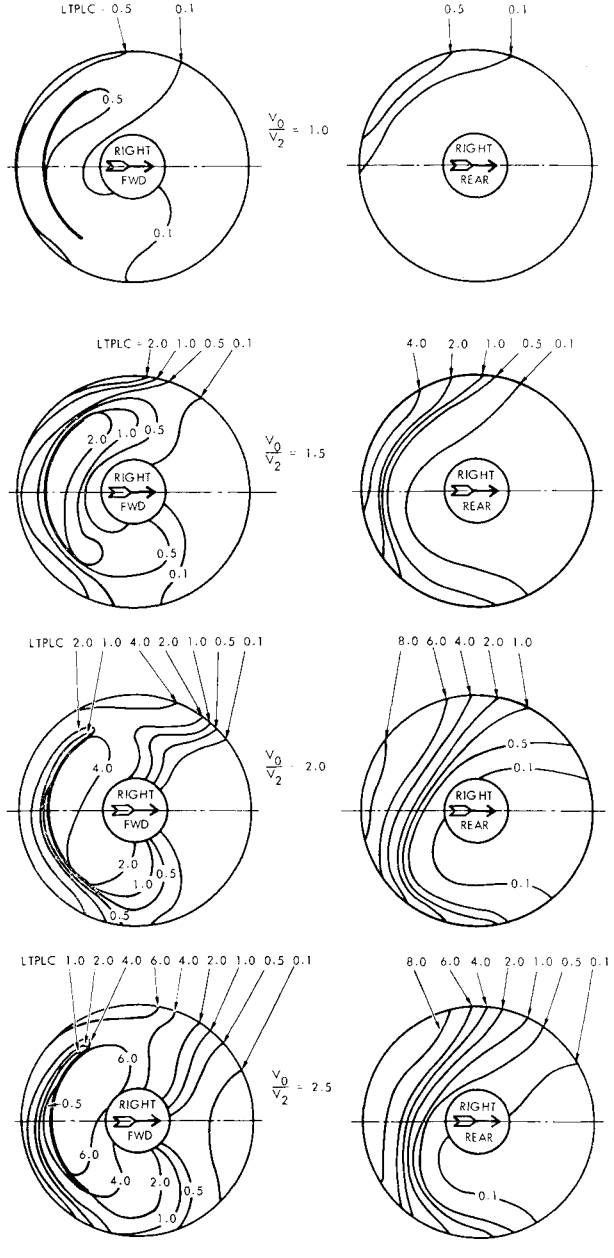


**Fig. 9 Distributions of total pressure loss for forward and rear inlets, final configuration, $\alpha = 10°$, $\beta = 0°$.**

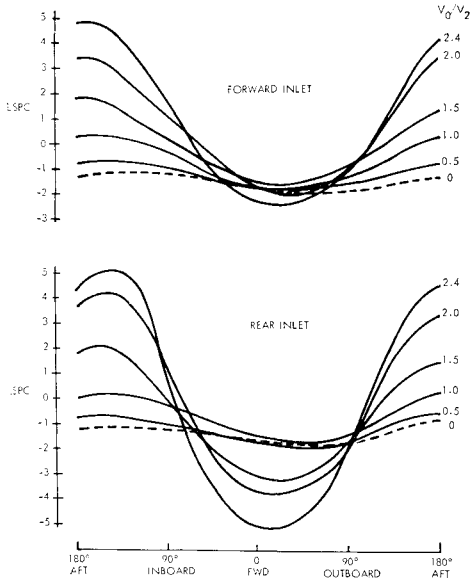


**Fig. 10 Circumferential distributions of local static pressure coefficient for final configuration with $\alpha = 10°$, $\beta = 0°$.**

centerline lip in the downwind rear inlets. In general, however, the losses at $\beta = -45°$ were again small in the range of freestream velocity of interest.

The local total pressure loss patterns given in Fig. 9 for $\alpha = 10°$, $\beta = 0°$ show that in the range $1.0 \leqq V_0/V_2 \leqq 2.5$ the characteristic flow separation and loss patterns develop giving progressively increasing areas and magnitudes of distortion. Tests at this condition but with $0 \leqq V_0/V_2 \leqq 0.5$, that is, at high power and relative wind speeds less than about 150 knots, indicated very low total pressure losses and distortions. It is important to note that the pressure loss magnitudes in the high loss zones are appreciably smaller for the forward inlet with the auxiliary lip than for the clean rear inlet. Further, it may also be significant from an engine operational standpoint that the peak loss zone occurs at smaller radii with the auxiliary lip. A very small peak loss zone was consistently detected outboard on the outer wall of the forward inlet. This small separation cavity probably originated from either the lip support strut attachment point or, less likely, from a separation on the relatively sharp outboard lip profile.

For all velocity ratios giving appreciable losses at zero sideslip, the pressure loss pattern is distorted, with higher losses outboard than inboard. The loss distributions for both the left and right forward inlets were examined at essentially identical test conditions and it was concluded that this distortion of the pattern is due to the relatively smaller lip radii outboard rather than due to an engine rotation effect. It was possible to conclude from this and other similar examinations that engine rotation had no significant effect on the pressure distortion patterns.

The circumferential static pressure plots (Fig. 10) show the powerful influence of $V_0/V_2$ on the distributions and particularly on the distortion of the pattern. It is notable that static pressures in the aft portions of all inlets are similar at all $V_0/V_2$ and increase with $V_0/V_2$ as a result of the ram effect. In contrast, the static pressures near the forward lips on the front and rear inlets are not similar. This dissimilarity is a result of the relatively constant streamtube area which is maintained between the basic and auxiliary lips in the front inlets. In this zone, the static pressure coefficient is approximately independent of $V_0/V_2$. In the clean rear inlets, however, the increased lip suction force required to turn the airstream at high values of $V_0/V_2$ causes the forward lip suctions in these inlets to increase markedly above about $V_0/V_2 = 1.5$.

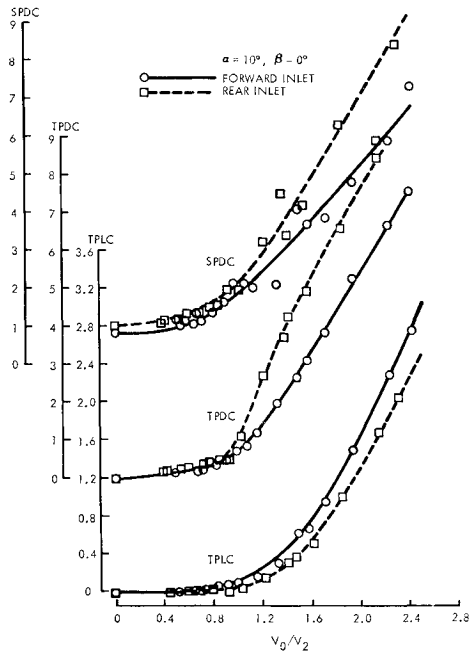


**Fig. 11 Typical test data for final inlet configuration.**

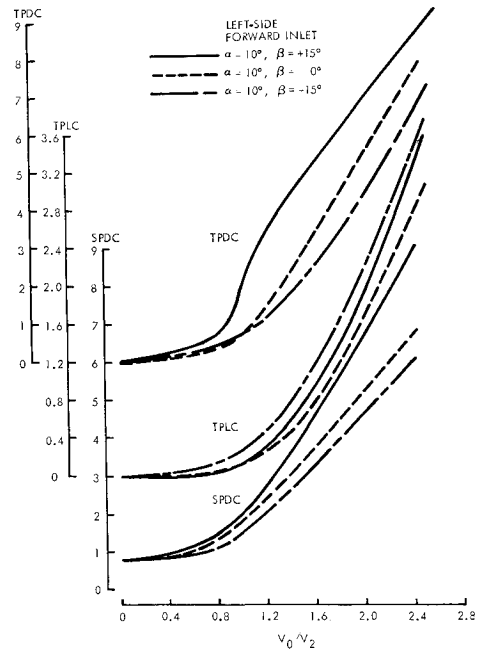


**Fig. 13 Typical effect of yaw on coefficients for final inlet configuration.**

The total and static distortion and loss coefficient data plotted vs $V_0/V_2$ (Figs. 11–13) show that, as expected, increasing freestream-to-inlet velocity ratio has a consistently adverse effect on TPLC as well as on TPDC and SPDC, as noted above. Figure 11 gives the test data for typical forward and rear inlets; the correlation of the data, obtained at the engine power and wind speed conditions given in Table 1, is shown to be excellent for both TPDC and TPLC. Although the SPDC data show appreciable scatter, this has been shown in Ref. 10 to be almost exclusively due to errors arising from the combination of the use of mercury manometers and the data collection and reduction process. It is notable that the forward inlet suffers greater pressure losses than the rear inlet despite the lower values of total pressure distortion indicated (Fig. 11).

The effect of pitch at high speeds is shown in Fig. 12. The plots indicate that for the forward inlets, pitch has very little effect. As expected from considerations of flow turning, a favorable effect is noted for nose-down attitudes and an adverse effect for nose-up attitudes.

The influence of yaw angle at high speeds is shown in Fig. 13. These data indicate that the upwind inlets ($\beta = +15°$) invariably suffer greater TPDC's than the zero yaw values but that downwind inlets ($\beta = -15°$) give reduced TPDC's.

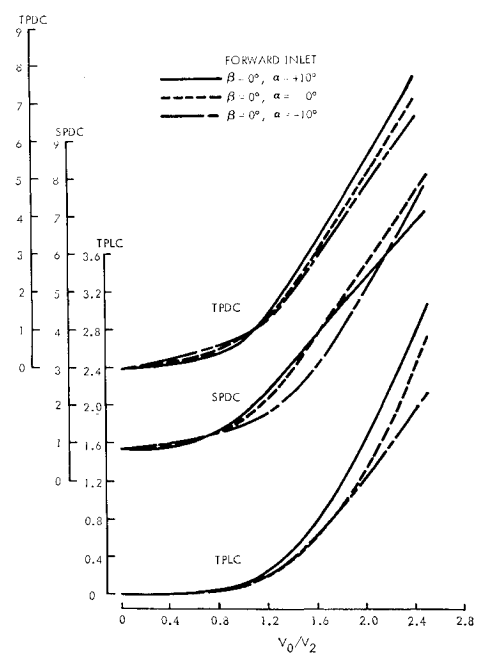


**Fig. 12 Typical effect of pitch on coefficients for final inlet configuration.**

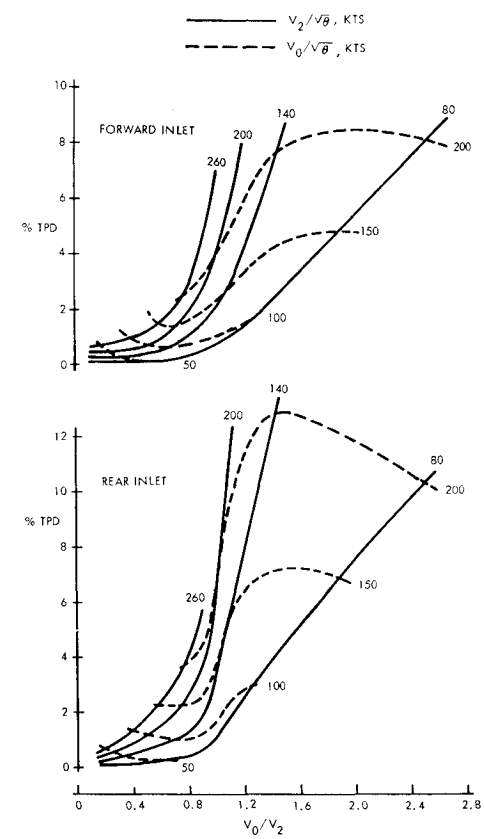


**Fig. 14 Total pressure distortion for final configuration, $\alpha = 10°$, $\beta = 0°$.**

Pressure losses do not follow this pattern; Fig. 13 shows that pressure losses in the forward inlet are greater with yaw than in symmetrical flight.

Figures 14 and 15 show plots of TPD and SPD obtained from the faired high-speed coefficient results for $\alpha = 10°$ and $\beta = 0°$; this condition most nearly corresponds with XV-4B transitional flight conditions.[9] The results indicate that for fixed values of $V_2$, corresponding to fixed engine speeds, TPD and SPD increase progressively with $V_0$. Although the effects of engine speed on TPD are variable and dependent upon $V_0/V_2$ and on the inlet location, the effect on SPD is invariable and SPD increases with increasing engine speed. Inlet velocities ($V_2$) of 80 and 260 knots represent approximately idle and maximum engine powers, respectively.

Figure 16 shows envelopes of TPD and SPD developed from Figs. 14 and 15 for typical accelerating or decelerating transitions at maximum and minimum weights. The plots show that TPD values approach the engine manufacturer's recommended limit of 10% only at airspeeds in excess of 180 knots on the rear inlet. The values of SPD are generally higher than the recommended limit of 5% but the engine manufacturer has reviewed the data and has indicated that these should not lead to engine operating problems. Confidence in the adequacy of the inlet design evolves from the fact that engine stalls and surges were absent throughout the program, and that numerous engine starts and accelerations at 200 knots relative wind speed were successfully accomplished. Also, engine vibration levels were always within the manufacturer's recommended limits. It is noted here that no data on SPD have been given by other investigators.[1-6]

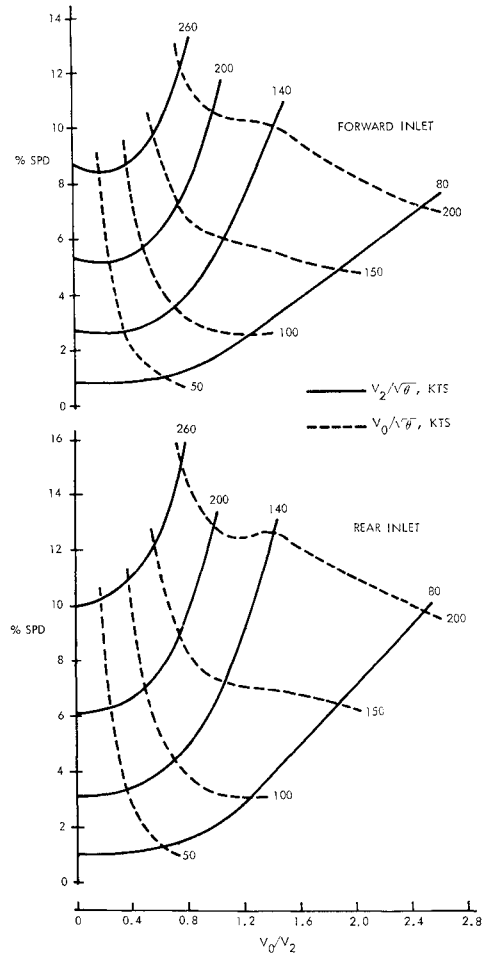


**Fig. 15 Static pressure distortion for final configuration, $\alpha = 10°$, $\beta = 10°$.**

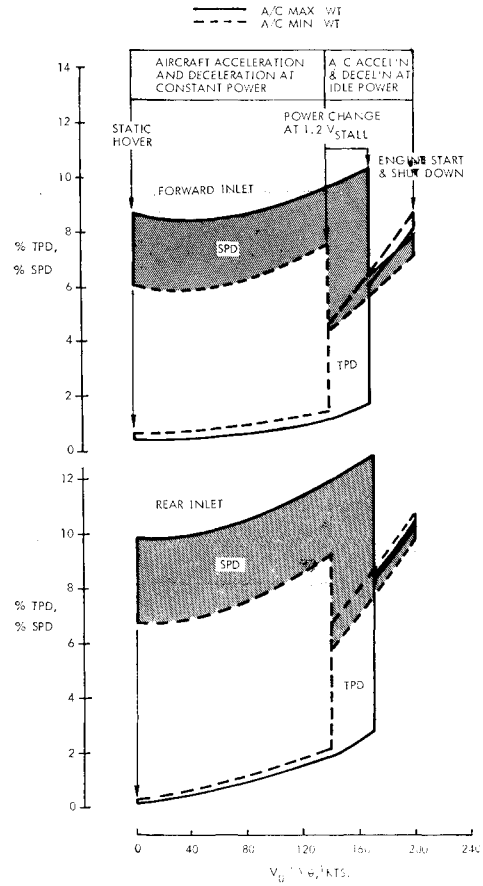


**Fig. 16 Envelopes of total and static pressure distortion for typical transition.**

## Concluding Remarks

Satisfactory lift engine inlet performance can be achieved with fixed inlet geometry. Single fixed auxiliary lips are required only in the forward inlets. Although this design feature was not fully optimized in this study, it showed sufficient promise to warrant consideration for the general class of vertical lift power plant installations.

Engine stalls, surges, and critical vibration levels were absent throughout the test program, which included numerous starts and accelerations at 200 knots relative wind speed. The critical pressure recovery at static hover conditions was optimum, while total and static pressure distortions were always less than 13% and generally less than 10% in the VTOL operational envelope. The independent influences of engine power and relative wind speed have been clearly displayed (Figs. 14 and 15), whereas their independent significance has not been emphasized by other investigators.

## References

[1] Simonetti, A. X., "Wind Tunnel Investigations of Air Inlets and Exhaust Systems for Lift Engines Located in Tandem," LR-16961, June 1963, Lockheed-California Co., Burbank, Calif.

[2] Tyson, B. I., "Tests to Establish Flow Distortion Criteria for Lift Engines," *Journal of Aircraft*, Vol. 2, No. 5, Sept.-Oct. 1965, pp. 411–417.

[3] Wiles, W. F., "Jet Lift Intakes," *Proceedings of an AGARD Fluid Dynamics Panel Conference on Aerodynamics of Power Plant Installation*, AGARDograph 103, pt. 2, Oct. 1965, Advisory Group for Aeronautical Research and Development, pp. 559–586.

[4] Tolhurst, W. H., Jr. and Kelly, M. W., "Characteristics of Two Large-Scale Jet-Lift Propulsion Systems," *Proceedings of Conference on V/STOL and STOL Aircraft*, SP-116, April 1966, NASA Ames Research Center, Moffett Field, Calif., pp. 205–228.

[5] Lavi, R., "Full-Scale Wind Tunnel Investigations of VTOL

Lift-Engine Inlet Performance and Operation," *Journal of Aircraft*, Vol. 4, No. 2, March-April 1967, pp. 125–132.

[6] Kirk, J. V. and Barrack, J. P., "Reingestion Characteristics and Inlet Flow Distortion of V/STOL Lift Engine Fighter Configurations," *Journal of Aircraft*, Vol. 6, No. 2, March–April 1969, pp. 116–122.

[7] Shumpert, P. K., Harris, A. E., and Picklesimer, E. A., "XV-4B Inlet Development Test Report," ER-9243, July 1967, Lockheed-Georgia Co., Marietta, Ga.

[8] Blackaby, J. R. and Watson, E. C., "An Experimental Investigation at Low Speeds of the Effects of Lip Shape on the Drag and Pressure Recovery of a Nose Inlet in a Body of Revolution," TN 3170, April 1954, NACA.

[9] "Propulsion/Performance/Stability and Control," *VTOL Integrated Handling Qualities Investigation Vehicle*, ETP 623, Vol. III, July 1965, Lockheed-Georgia Co., Marietta, Ga.

[10] Shumpert, P. K. and Harris, A. E., "Full-Scale V/STOL Lift Engine Inlet Development Tests," ER-9663, Vol. I–III, April 1968, Lockheed-Georgia Co., Marietta, Ga.

JULY-AUG. 1969 J. AIRCRAFT VOL. 6, NO. 4

# A Control System Concept for an Axisymmetric Supersonic Inlet

K. S. CHUN* AND R. H. BURR†
*The Boeing Company, Seattle, Wash.*

**A control system concept for the operation of an axisymmetric supersonic inlet in a mixed compression mode is described, and the test results to substantiate the soundness of the concept are presented. The control system consisted of a centerbody control loop, a normal shock control loop, and a restart control loop. The analytical considerations and wind-tunnel test data leading to the selection of the control pressure signals required for the system are discussed. The control loop tests were conducted at a number of selected Mach numbers from 2.0 to 2.6 on two 11.24-in.-lip variable-geometry inlets. All control loop components, except the close-coupled pressure transducers, the hydraulic servovalves, and the actuators, were simulated on an analog computer. Control loop responses were evaluated as the Mach number, the inlet angle of attack, and the downstream airflow were varied in both ramp and sinusoidal forms. The inlet restart control function was also evaluated. The test results indicated that the control system concept, with the selected control signals, satisfactorily meets the control requirements of the mixed compression mode.**

## Nomenclature

| | |
|---|---|
| $Ap$ | = exit plug area |
| $E_B$ | = integrator limit |
| $E_{CB},E_{NS}$ | = error signals |
| $G_{CB}(s),G_{NS}(s),G_{SB}(s)$ | = pneumatic line dynamics |
| $K_{BY},K_{CB}$ | = loop gains |
| $M_L$ | = Mach number ahead of inlet |
| $M_{TH}$ | = inlet throat Mach number |
| $P_C$ | = restart control pressure |
| $P_{CB}$ | = centerbody control pressure, cowl static |
| $P_{CBM}$ | = centerbody control pressure, manifolded cowl static |
| $P_{CS}$ | = cowl static pressure |
| $P_{TL}$ | = tunnel total pressure |
| $P_{NS}$ | = normal shock control pressure |
| $P_{SB}$ | = shock-bias control pressure |
| $P_{TNS}$ | = throat total pressure |
| $P_{T2}$ | = compressor face total pressure |
| $PR$ | = control pressure ratio |
| $R_{CB}$ | = centerbody radius |
| $s$ | = Laplace operator |
| $T_{CB},T_{NS}$ | = time constants |
| $\alpha$ | = inlet angle of attack |
| $\theta$ | = circumferential angle |

Presented as Paper 68-581 at the AIAA 4th Propulsion Joint Specialist Conference, Cleveland, Ohio, June 10–14, 1968; submitted August 5, 1968; revision received April 11, 1969.

* Senior Group Engineer, Inlet Controls, Propulsion Staff, Supersonic Transport Branch.

† Research Engineer, Propulsion Staff, Supersonic Transport Branch. Member AIAA.

## Introduction

SUPERSONIC aircraft with a high Mach number cruise condition must employ variable-geometry inlets with an efficient control system to achieve high performance and stable airflow for the engine. Rapid geometry changes for stable operation during environmental turbulence, engine transients, and airplane maneuver are among the most critical requirements for the inlet control system.

This requirement is quite severe for mixed compression inlets because the shock system is sensitive to many variables. Therefore, a major effort must be made to develop a control system that will sense these variables and provide fast response. This paper presents a control system concept found to be satisfactory for the operation of an axisymmetric

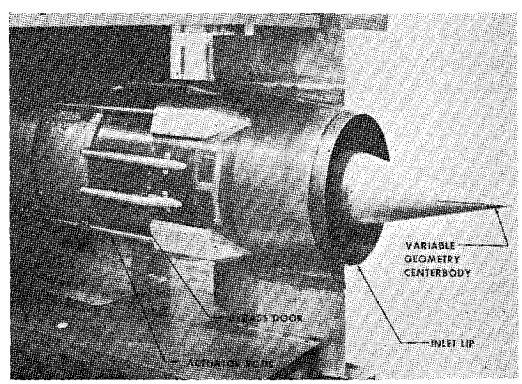


**Fig. 1 11.24-in. variable-geometry inlet model.**